

# Quasi-isotropic 3-D resolution in two-photon scanning microscopy

Cristina Ibáñez-López<sup>+</sup>, Genaro Saavedra<sup>+</sup>, and Gilbert Boyer

Laboratoire d'Optique Appliquée, Ecole Polytechnique–Ecole Nationale Supérieure de Techniques Avancées, Centre de l'Yvette, Chemin de la Hunière, 91761 Palaiseau, France

<sup>+</sup> Permanent address: Departamento de Óptica, Universidad de Valencia, E46100 Burjassot, Spain  
[Cristina.Ibanez@uv.es](mailto:Cristina.Ibanez@uv.es), [Genaro.Saavedra@uv.es](mailto:Genaro.Saavedra@uv.es), [Boyer.Gilbert@neuf.fr](mailto:Boyer.Gilbert@neuf.fr)

Manuel Martínez-Corral

Departamento de Óptica, Universidad de Valencia, E46100 Burjassot, Spain  
[Manuel.Martinez@uv.es](mailto:Manuel.Martinez@uv.es)

**Abstract:** One of the main challenges in three-dimensional microscopy is to overcome the lack of isotropy of the spatial resolution, which results from the axially-elongated shape of the point spread function. Such anisotropy gives rise to images in which significant axially-oriented structures of the sample are not resolved. In this paper we achieve an important improvement in z resolution in two-photon excitation microscopy through spatial modulation of the incident beam. Specifically, we demonstrate that the design and implementation of a simple shaded ring performs quasi-isotropic three-dimensional imaging and that the corresponding loss in luminosity can be easily compensated by most available femtosecond lasers. The outcome looks particularly relevant to nano-fabrication and optical manipulation.

© 2005 Optical Society of America

**OCIS Codes:** (180.5810) Scanning microscopy; (1000.6640) Superresolution; (100.1220) Apertures.

---

## References and Links

1. Abbe, E. *Arch. Mikrosk. Anat.* **9**, 413–468 (1873).
2. T. R. M. Sales, "Smallest focal spot," *Phys. Rev. Lett.* **81**, 3844–3847 (1998).
3. J. Miao, T. Ishikawa, B. Johnson, E. K. Anderson, B. Lai and K. O. Hodgson, "High resolution 3D x-ray diffraction microscopy," *Phys. Rev. Lett.* **89**, 088303 (2002).
4. J. Miao, T. Ohsuna, O. Terasaki, K. O. Hodgson and M. A. O'Keefe, "Atomic resolution three-dimensional electron diffraction microscopy," *Phys. Rev. Lett.* **89**, 155502 (2002).
5. C. M. Blanca and S. W. Hell, "Axial superresolution with ultrahigh aperture lenses," *Opt. Express* **10**, 893–898 (2002).
6. J. B. Pawley, ed., *Handbook of biological confocal microscopy*. Plenum Press, New York, 1995.
7. The term superresolution introduced here is understood in the sense of Rayleigh criterion; i. e., as the narrowness of the PSF or, equivalently, the enhancement of the OTF for frequencies under the cut-off frequency.
8. S. Lindek, J. Swoger and E. H. K. Stelzer, "Single-lens theta microscopy: resolution, efficiency and working distance," *J. Mod. Opt.* **46**, 843–858 (1999).
9. B. Bailey, D. L. Farkas, D. Lansing-Taylor and F. Lanni, "Enhancement resolution in fluorescence microscopy by standing-wave excitation," *Science* **366**, 44–48 (1993).
10. J. Huisken, J. Swoger, F. Del Bene, J. Wittbrodt and E. H. K. Stelzer, "Optical sectioning deep inside live embryos by selective plane illumination microscopy," *Science* **305**, 1007–1009 (2004).
11. M. A. A. Neil, R. Juskaitis, T. Wilson, Z. J. Laczik and V. Sarafis, "Optimized pupil-plane filters for confocal microscope point-spread function engineering," *Opt. Lett.* **25**, 245–247 (2000).
12. C. J. R. Sheppard, "Binary optics and confocal imaging," *Opt. Lett.* **24**, 505–506 (1999).
13. M. Martínez-Corral, M. T. Caballero, E. H. K. Stelzer and J. Swoger, "Tailoring the axial shape of the point spread function using the Toraldo concept," *Opt. Express* **10**, 98–103 (2002).
14. G. Boyer, "New class of axially apodizing filters for confocal scanning microscopy," *J. Opt. Soc. Am. A* **19**, 584–589 (2002).
15. M. Martínez-Corral, C. Ibáñez-López, G. Saavedra and M. T. Caballero, "Axial gain in resolution in optical sectioning fluorescence microscopy by shaded-ring filters," *Opt. Express* **11**, 1740–1745 (2003).
16. S. S. Sherif and P. Török, "Pupil plane masks for super-resolution in high-numerical-aperture focusing," *J. Mod. Opt.* **51**, 2007–2019 (2004).

17. W. Denk, J. H. Strickler and W. W. Webb, "Two-photon laser scanning fluorescence microscopy," *Science* **248**, 73-76 (1990).
18. C. M. Blanca, J. Bewersdorf and S. W. Hell, "Single sharp spot in fluorescence microscopy of two opposing lenses," *Appl. Phys. Lett.* **79**, 2321-2323 (2001).
19. T. A. Klar, S. Jakobs, M. Dyba, A. Egner and S. W. Hell, "Fluorescence microscopy with diffraction resolution barrier broken by stimulated emission," *Proc. Natl. Acad. Sc.* **97**, 8206-8210 (2000).
20. M. Dyba and S. W. Hell, "Focal spots of size  $\lambda/23$  open up far-field fluorescence microscopy at 33 nm axial resolution," *Phys. Rev. Lett.* **88**, 163901 (2002).
21. C. Ibáñez-López, I. Escobar, G. Saavedra and M. Martínez-Corral, "Optical sectioning improvement in two-color excitation scanning microscopy," *Microsc. Res. Tech.* **64**, 96-102 (2004).
22. The eccentricity is defined here as  $e = \sqrt{1 - b^2/a^2}$ , where a and b account for the lengths of the semimajor and semiminor axes, respectively.
23. S. Kawata, H.-B. Sun, T. Tanaka and K. Takada, "Finer features for functional microdevices," *Nature* **412**, 697-698 (2001).
24. D. G. Grier, "A revolution in optical manipulation," *Nature* **424**, 810-816 (2003).
25. B. Richards and E. Wolf, *Proceedings of the Royal Society (London) A* **253**, 358 (1959).
26. P. Török and P. Varga, "Electromagnetic diffraction of light focused through a stratified medium," *Appl. Opt.* **36**, 2305-2312 (1997).
27. O. Haeberlé, "Focusing of light through a stratified medium: a practical approach for computing microscope point spread functions. Part I: Conventional microscopy," *Opt. Commun.* **216**, 55-63 (2003).

## 1. Introduction

The spatial resolution of imaging systems is mainly restricted by diffraction, that is, by their capacity for producing a tight diffraction spot when imaging a light point source. Since Abbe formulated his wave theory for microscopic imaging [1], the improvement of resolution of optical microscopes has been the aim of many research efforts. The need for smaller spot sizes is desirable, not only in the case of optical frequencies [2], but also in other spectral ranges like x-ray microscopy [3] or electron microscopy [4]. In the search for the maximum resolution, emphasis has been generally placed on the use of modern microscope objectives with the highest available numerical aperture (NA) [5]. But even with the best optical elements the use of wide-field conventional optical microscopes to image three-dimensional (3-D) biological fluorescent samples has the drawback that any image focused at a certain depth in the sample contains blurred information from the rest of the sample. This fact gives rise to 3-D images with deteriorated contrast.

To overcome this problem, the use of scanning fluorescence techniques has been demonstrated and routinely used. Among them we cite first single-photon confocal microscopes (SPCM). The main advantage of SPCM is its sectioning power, due to the light rejection from out-of-focus parts of the sample [6]. But since the diffraction pattern of a focused bright spot is naturally prolate shaped for any NA, SPCM suffers from anisotropic imaging. As a specific feature, super-resolving apodization [7] can be considered complementary and compatible to many other approaches for reducing the imaging anisotropy such as confocal theta microscopy [8], standing wave microscopy [8], or selective plane illumination microscopy [10]. Apodization has been the subject of increased interest in the past few years due to the demands of data storage, nano-fabrication and optical manipulation. Filters designed to obtain a moderate gain in resolution remain easy to implement, despite the strong unbalance between the few experimental results and the many theoretical solutions, among which continuous, binary, purely-absorbing, complex-transmittance and, more recently, purely-dephasing filters have been proposed [11-16].

A serious drawback of SPCM is photobleaching, which occurs since the entire sample is bleached when any single plane is imaged. Another drawback of this technique when used in biomedical imaging is its poor depth-penetration capacity. To solve these problems, two-photon excitation (TPE) scanning microscopy was demonstrated [17]. This non-linear imaging technique relies on the simultaneous absorption of two photons, whereby a single fluorescence photon is emitted. The overall fluorescent light is collected and finally the image is synthesized from the 3-D sampling of the object. TPE generally uses near-infrared light due to its lower absorption and scatter in biological tissues, which allows deeper penetration of the excitation beam. Besides, photobleaching is restricted to the neighborhood of the imaged plane.

Several attempts have been made to improve the axial resolution of TPE scanning microscopes. This is the case of 4Pi microscopes in which two opposing, high-NA objectives are used to create an interference illumination spot with very narrow axial central lobe [18], or the combination between STED microscopy and 4Pi microscopy [19,20].

To implement the above-cited methods a strong modification of the TPE microscope architecture is needed. Specifically, the need for multiple objectives makes the system alignment a very complicated issue. Here we concentrate on apodization of the TPE mode with the aim of reducing anisotropic imaging, by pupil spatial filtering with a shaded-ring filter (SR) [21], often dubbed leaky filter. We demonstrate that a close to spherical 3-D PSF can be obtained through the implementation of a relatively inexpensive spatial filter. Interestingly, the measured PSF has no significant collateral enhancement of secondary lobes, and lateral broadening of the central core is not observed. Approximated as an ellipsoid, the engineered PSF exhibits an eccentricity reduced from  $e=0.72$  to  $e=0.48$  [22]. The quasi-spherical spot can be very useful not only for micro-imaging applications, but also in other techniques like nanofabrication [23] or optical manipulation [24].

## 2. Description of the method

To describe our approach, we start by considering a monochromatic, linearly-polarized plane wave that impinges on an aberration-free high-aperture spherical lens. Assuming that sine condition holds, and according to electromagnetic focusing theory of Richards and Wolf [25], the electric field distribution in the focal region is given by

$$\mathbf{E}(r, z, \varphi) = [I_0(r, z) + I_2(r, z)\cos 2\varphi]\mathbf{i} + I_2(r, z)\sin 2\varphi\mathbf{j} + i2I_1(r, z)\cos \varphi\mathbf{k} \quad (1)$$

where

$$I_0(r, z) = \int_0^\alpha P(\theta)\sqrt{\cos\theta} (1 + \cos\theta) J_0(kr\sin\theta) \exp(ikz\cos\theta) \sin\theta d\theta$$

$$I_1(r, z) = \int_0^\alpha P(\theta)\sqrt{\cos\theta} \sin\theta J_1(kr\sin\theta) \exp(ikz\cos\theta) \sin\theta d\theta \quad (2)$$

$$I_2(r, z) = \int_0^\alpha P(\theta)\sqrt{\cos\theta} (1 - \cos\theta) J_2(kr\sin\theta) \exp(ikz\cos\theta) \sin\theta d\theta$$

In the above equations,  $P(\theta)$  accounts for the amplitude transmittance at the aperture stop of the focusing lens, whereas  $\alpha$  is the maximum value of the aperture angle  $\theta$ . Parameter  $\varphi$  represents the angle between the polarization direction of the incident field (assumed  $x$ -direction) and the observation meridian plane. More accurate calculations should take into account the influence of the transmission coefficients of the various interfaces inherent to the stacked structures commonly used in microscopy [26, 27]. However, the use of these more accurate models would not change significantly the results. Even if the illumination setup is not telecentric, TPE scanning microscopes are 3-D linear and shift-invariant systems due to their scanning nature, provided that the illumination spot is not affected by spherical aberration when going deeper into the specimen. Therefore, the image can be described as the convolution between the 3-D PSF and the 3-D function that describes the spatial distribution of fluorescence generated by the object. If we consider that, in the optimum case, no photobleaching affects the sample and no saturation effects occur, then the PSF is given by

$$\text{PSF}(r, z, \varphi) = |\mathbf{E}(r, z, \varphi)|^4. \quad (3)$$

Our aim here is the design and production of elements that narrow the PSF along the axial direction. The narrowness should be produced at the expense of neither a deterioration of the

lateral resolution nor an enlargement of axial sidelobes. The utility of SR filters has been demonstrated, only by numerical simulations, in single-photon confocal microscopy [15]. Here we adapt the SR concept to TPE and experimentally demonstrate, for the first time, their capacity for producing 3-D superresolution. The design of the proper SR filter must take into account the lens NA and the illumination polarization state. In our experiment we used as the illumination source a mode-locked Cr<sup>4+</sup>:fosterite laser. The laser produced pulses with central wavelength  $\lambda = 1260$  nm and a mean temporal width  $\Delta t = 50$  fs at a repetition rate of 84 MHz. An average power over 200 mW was available for the experiment. The polarization of the beam was rigorously linear. In our analysis we set the coordinate system so that the incident light is seen as *x*-polarized. For the illumination and collection we used two identical 1.2 NA (water-immersion) objectives from Olympus (Uplan APO/IR 60X). The maximum gain in axial resolution that can be, theoretically, achieved with purely absorbing screen 1.73. But this ideal gain is achieved at the expense of blocking all incident light. When realistic experiments are considered, the maximum gain achievable is about 1.30. In our case we selected 1.25 as the value of the gain in axial resolution. As the result of the optimization procedure we de-

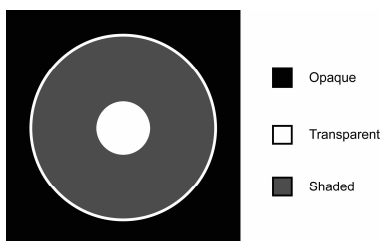


Fig. 1. Amplitude transmittance of the SR filter. The transmittance of the shaded ring is 19%.

signed the SR filter that maximizes the light-spot efficiency (evaluated as the fluorescence intensity emitted from the central lobe divided by the overall fluorescence intensity). The filter is shown in Fig. 1. At opening between  $\theta_1 = 15^\circ$  and  $\theta_2 = 62^\circ$  the amplitude transmittance of the designed filter is 19% .

In Fig. 2 we compare the, numerically evaluated, PSFs corresponding to the standard 1.2 NA objective, with the one in which the SR filter is inserted as the aperture stop. The calculations were performed according to Eq. (3), for the case of  $\varphi=0$ . These calculations predict: (a)

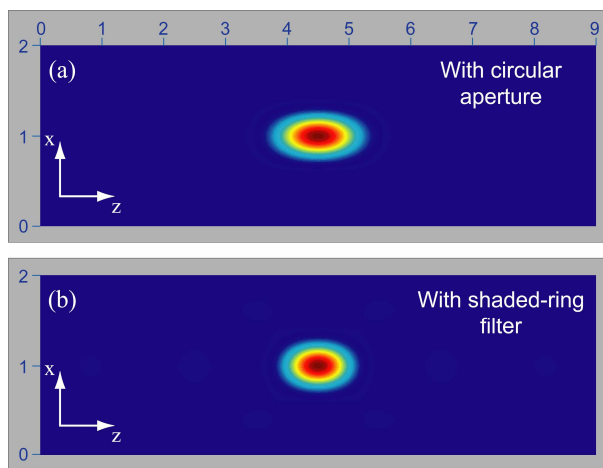


Fig. 2. Plot of the numerically evaluated 3-D PSF, in the meridian plan  $\varphi = 0$ , corresponding to: (a) Standard 1.2 NA objective with clear pupil; and (b) Same objective but with the SR filter inserted as the aperture stop. Axes labels are expressed in microns.

length reduction of the PSF by 21% (as evaluated in terms of the full-width at half maximum (FWHM)); (b) a very small lateral swelling (4% in terms of FWHM); and (c) a very low dimming of the light-spot efficiency, which decreases from 99% for the clear-aperture to 87% for the proposed SR.

### 3. Experimental results

In Fig. 3 we show a scheme of the experimental setup. The laser output beam was expanded to overfill the illumination-lens pupil, and carefully positioned and oriented through a periscopic mirror arrangement. To prevent bleaching, the average light power incident on the sample was kept under 6 mW by a set of neutral-density filters. Just in front of the objective we inserted the SR filter. The emitted fluorescence light due to the two-photon excitation was collimated by the collector lens. A RG630 filter blocked the transmitted pump light. The signal was detected by a GaAs photo-multiplier tube (PMT) and processed by a lock-in amplifier. The sample consisted of Dark-Red stained beads of 200 nm in diameter embedded in an index-matched filling medium and stuck on one coverslip. We used a solution of latex microspheres loaded with dark red fluorescent dye (Molecular Probes). To prepare the samples, first of all we placed a drop of acetone mixed with cello-tape on an oil and dust-free slide. After the acetone dries, we added a drop of water-diluted solution of beads. Before sampling, the dilution was sonicated to ensure that the beads were uniformly suspended. We wait for the droplet to dry and then we apply a drop of water over the dry sample of beads. Finally we cover the sample with a coverslip which is sealed with nail polish. The position of the sample was controlled with a precision of a few nanometers. Due to the vectorial nature of the, the PSF has not cylindrical symmetry. As it is well-known, the PSF is wider in the direction perpendicular to the incident polarization. For this reason, we performed a  $x$ - $z$  raster scanning through a centered section of the bead. Due to the ellipsoidal shape of the PSFs, the spacing for the scanning was different in the  $x$ -direction (33 nm) than in the  $z$ -direction (90 nm). An important point to address here is the need for a second objective for the collection of the fluorescence. Although the presence of this second objective seems to make the system more sensible to misalignments, its use is necessary, because the use of the SR filter in detection would decrease strongly the collection efficiency. This fact would reduce significantly the values of the axial gain that could be used, and therefore would play strongly against the aim of this research. Note on the other hand that having the second objective not imaging but simply detecting functions, the problems of alignment are simplified.

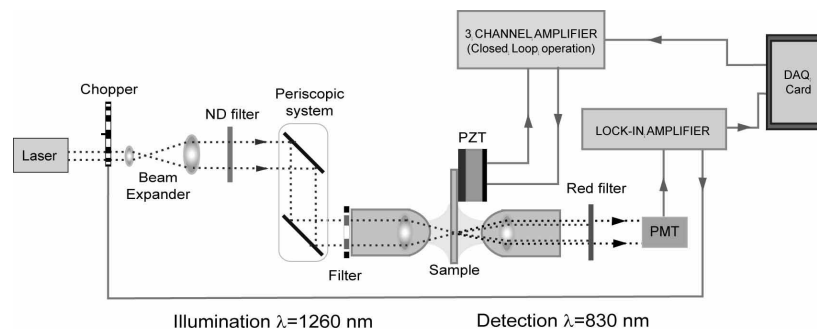


Fig. 3.- Schematic geometry of the TPE scanning microscope.

In Fig. 4 we present typical results for the PSF measurements obtained with and without the SR filter. The PSF obtained with the SR is clearly narrowed along the optical-axis direction, thus exhibiting close to spherical shape. After the comparison between these results and the numerical ones, and taking into account that what indeed was measured is the convolution between the PSF and the bead, we find a good agreement between them.

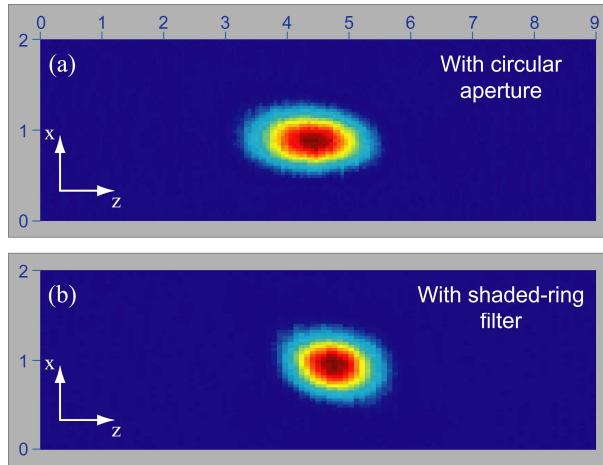


Fig. 4.- 2D gray-scale sections of the experimental 3-D PSFs as displayed by LabView. (a) PSF obtained with the standard 1.2 NA objective with clear pupil; and (b) PSF obtained with the same objective but with the SR filter inserted as the aperture stop.

To get a better insight into the experimental results, we have plotted, in Fig. 5, the axial and lateral profiles of the above measured PSFs. Note from this figure that no significant dilation is produced in the lateral direction. However, the axial FWHM is reduced from  $1.43 \mu\text{m}$  to  $1.13 \mu\text{m}$ . Since the lateral FWHM is, in both cases, about  $0.99 \mu\text{m}$ , the eccentricity of the 3-D PSF is reduced by 33%.

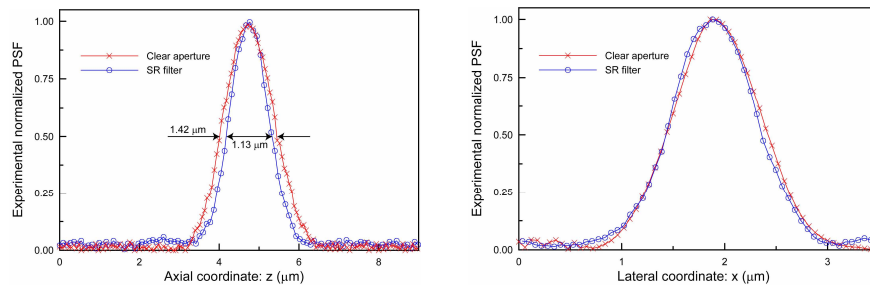


Fig. 5.- Normalized axial and lateral PSF produced by the Olympus 1.2 NA objective (x). With empty dots (o) we show the experimental results obtained when the SR filter is inserted in the illumination path.

#### 4. Conclusions

In summary, we have demonstrated that quasi-isotropic 3-D resolution can be produced in TPE scanning microscopy by spatial modulation of the illumination beam, which involves a small modification of the microscope architecture. The proposed amplitude modulator, the SR filter, has a very simple structure: a shaded ring centered in the objective aperture stop. We have implemented the filter in a quite simple manner, and obtained the quasi-spherical spot using a conventional TPE scanning architecture. The outcome can be very useful not only in 3-D microscopy, but also in nano-fabrication and optical manipulation. The experimental results are in quite good agreement with the theoretical predictions.

#### Acknowledgments

The authors wish to acknowledge stimulating discussions with Dr. P. Török (Imperial College, London). We also acknowledge Dr. K. Plamann for his help with the signal-processing software. We are also indebted to an anonymous, for his/her comments and suggestions,

which indeed help to improve the paper. This work was conducted in the frame of the Acción Integrada HF2003-0257, Ministerio de Ciencia y Tecnología, Spain and the Action Intégrée 07181VG Ministère des Affaires Etrangères, France, and mainly funded by the Plan Nacional I+D+I (grant DPI2003-4698), Ministerio de Ciencia y Tecnología and by the Generalitat Valenciana, Spain (Grant GV04B-186).